Deep Sea Research Part I: Oceanographic Research Papers
December 2005; 52(12) : 2275-2284
http://dx.doi.org/10.1016/j.dsr.2005.09.001

Assessments of anthropogenic CO2 distribution in the tropical Atlantic Ocean

F. Touratier[a*], C. Goyet[a], C. Coatanoan[b] and C. Andrié[c]

[a]BDSI, Université de Perpignan Via Domitia, 52 avenue Paul Alduy, 66860 Perpignan, France
[b]IFREMER, Centre de Brest, BP 70, 29280 Plouzané, France
[c]LODYC, CNRS/IRD/Université Pierre et Marie Curie, 4 place Jussieu, case 100, 75252 Paris Cedex 05, France

*: Corresponding author : Tel.: +33 4 68661744; fax: +33 4 68662144. touratie@univ-perp.fr

Abstract: With a limited number of properties (salinity, temperature, total dissolved inorganic carbon, total alkalinity, and oxygen) from a recent cruise in the tropical Atlantic Ocean, we use the simple and recent approach TrOCA (Tracer combining Oxygen, inorganic Carbon, and total Alkalinity) to estimate the distribution of anthropogenic CO2 along three latitudinal sections. In order to assess the quality of the anthropogenic CO2 distribution, results from the method are compared to the CFC-11 measurements. We discuss the large-scale distribution of the main water masses of the tropical Atlantic Ocean in the light of the anthropogenic CO2 and the CFC-11 distributions. Keeping in mind that the anthropogenic CO2 emission began not, vert, similar60 years earlier than that of CFC-11, the former provides new insight on the local circulation and efficiency of the tropical waters to store the atmospheric carbon.

Keywords: Carbon cycle; Water mass; Atlantic Ocean; Tropical belt

Introduction

Since the early 1980's, several interdisciplinary programs and associated cruises (TTO, Transient Tracers in the Oceans, http://cdiac.esd.ornl.gov/oceans/ndp004.html; FOCAL, programme Français Océan Climat Atlantique Equatoriale, http://www.ifremer.fr/sismer/; CITHER 1, Circulation Thermohaline, http://www.ifremer.fr/sismer/; ETAMBOT 1 and 2, Etude du Transfert Atlantique Méridien dans le Bassin Ouest Equatorial; http://www.ifremer.fr/sismer/; EQUALANT 99 and 2000, Equatorial Atlantic, http://www.ifremer.fr/sismer/) have been organized to sample the tropical belt of the Atlantic Ocean. This area is characterized by a complex mesoscale circulation pattern where several equatorial deep jets are surrounded by columns of extra equatorial jets (Gouriou et al., 2001). At a larger scale, the circulation appears to be strongly influenced by the Deep Western Boundary Current (DWBC) which transports, southward and then eastward, the waters originating from the north. Whatever the scale of observation, the anthropogenic tracers, such as the chlorofluorocarbons (CFCs), have been shown to be particularly useful to unravel the complexity of the local circulation (e.g. Weiss et al., 1985; Rhein et al., 1995; Andrié et al., 1999).

Although the Atlantic Ocean as a whole is a strong CO_2 sink (Takahashi et al., 2002), most of area between 5°N and 5°S is a source of CO_2 for the atmosphere (Oudot and Andrié, 1986). This feature of the tropical waters stimulates research efforts on the carbon cycle in the area, efforts which are partially motivated by the conclusion of Goyet et al. (1998) that after a period of 10 years, the source of CO_2 substantially decreased because of the overall atmospheric CO_2 increase. In this context, the knowledge of the water column distribution of the anthropogenic CO_2 is particularly interesting since it gives information on the real efficiency of the ocean to store the excess carbon from the atmosphere.

Here we propose to use the results of the recent EQUALANT cruise (1999) to estimate the water column concentrations of anthropogenic CO_2 and to explore the influence of the large scale circulation on the distribution along three latitudinal sections. To compute the anthropogenic CO_2, we use the model recently developed by Touratier and Goyet (2004b). The results are discussed and compared in the light of the CFC-11 distribution, which provides an independent test of the quality of the estimate.

Data

The EQUALANT 1999 cruise (hereafter EQ99), aboard the oceanographic vessel R.V. Thalassa, occurred from 12 July to 22 August 1999 in the tropical Atlantic Ocean. As part of the French national program ECLAT (a component of the international program CLIVAR), one of the objectives of EQ99 was to study the deep circulation within the tropical region by measuring multidisciplinary properties of the water masses in the area. A total of 103 stations were sampled along three main sections, at 35°W, 23°W, 10°W, and two short sections, at 5°S and 7°W (Fig. 1).

In the present paper, we use salinity (S), potential temperature (θ; °C), oxygen (O_2; µmol kg^{-1}), total dissolved inorganic carbon (TCO_2; µmol kg^{-1}), and total alkalinity (TA; µmol kg^{-1}) to estimate the distribution of anthropogenic CO_2 (C_{ANT}; µmol kg^{-1}) with the TrOCA (Tracer combining Oxygen, inorganic Carbon, and total Alkalinity) approach. In order to assess the uncertainty of the results, the measured concentration of the anthropogenic tracer trichloro-fluoro-methane (CFC-11; pmol kg^{-1}) is further used for comparison with the distributions of estimated C_{ANT}.

CFC-11 measurements were performed by the classical extraction / trapping / gaz chromatography method described in Andrié et al. (2002). The detection limit is 0.006 pmol

kg^{-1} which is considered as the accuracy of the method for deep samples (for concentrations lower than 0.6 pmol kg^{-1}). The precision is around 1% of the measured values for surface and subsurface samples.

The methodology used to analyze the dissolved O_2 is similar to that described in the WOCE handbook (1994). This technique has been used for several cruises in the tropical Atlantic Ocean (CITHER 1, ETAMBOT 1 and 2; for details, see Billant and Branellec 1994, Fournier et al. 1997). The accuracy of O_2 measurements during EQ99 averages 0.44 µmol kg^{-1}.

Measurements of TCO_2 and TA were done by potentiometric acid titration. The principle of measurements as well as a complete description of the system used to perform accurate measurements can be found in the DOE handbook of methods for CO_2 analysis (DOE, 1994). The accuracy of the TCO_2 measurements, based on measurements of reference material provided by Dr. A. G. Dickson, was close to 1.3 µmol kg^{-1}. The precision of the TA measurements was close to 1.7 µmol kg^{-1} (EQUALANT 99 Cruise Report, 2000). A detailed analysis of the measurements performed after the EQ99 cruise reveals an important bias of ca. 12.7 µmol kg^{-1}in the TA data compared with those of the WOCE A15 section sampled in 1994 (called section WOCE A15/94; see Figs. 1 and 2) . Consequently, in order to calculate accurate values of anthropogenic CO_2, all TA original values are lowered by 12.7 µmol kg^{-1} (this corresponds to an increase of 6.35 µmol kg^{-1} for C_{ANT}).

Method to estimate the anthropogenic CO_2 content: the TrOCA approach

Three major kinds of models have been proposed to separate the anthropogenic signal from the bulk of TCO_2: 1) ocean circulation models coupled with modules describing the marine chemistry and the biology (e.g. Maier-Reimer, 1993; Stocker et al., 1994; Sarmiento et al. 1995); 2) simple time difference in TCO_2 concentrations (Peng et al., 1998); and 3) models using back calculation techniques (Brewer, 1978; Chen & Millero, 1979; Gruber et al., 1996; Goyet et al., 1999; Touratier and Goyet 2004b). The method used here belongs to the last type of model which provides the most precise estimates of anthropogenic CO_2 distribution. Among the existing back calculation techniques, the TrOCA approach (Touratier and Goyet, 2004a, b) is chosen for two main reasons: first, the method is very simple and easy to use; second, it has been successfully applied to estimate the anthropogenic CO_2 throughout the whole Atlantic Ocean (Touratier and Goyet, 2004b) and along a section of the southern ocean between South Africa and Antarctica (Lo Monaco et al., in press).

The TrOCA approach is based on the 'quasi-conservative' tracer TrOCA (Tracer combining Oxygen, inorganic Carbon, and total Alkalinity; see Touratier and Goyet, 2004a). It is defined by the relationship:

$$\mathrm{TrOCA} = \mathrm{O_2} + 1.2\,\mathrm{TCO_2} - 0.6\,\mathrm{TA} \qquad (1)$$

TrOCA has been shown to deviate significantly from conservation where waters are thought to be contaminated with anthropogenic CO_2 in the Atlantic Ocean (Touratier and Goyet, 2004a, b). The 'conservative' tracer $TrOCA^0$ is then defined as follows:

$$\mathrm{TrOCA}^0 = \mathrm{O_2^0} + 1.2\,\mathrm{TCO_2^0} - 0.6\,\mathrm{TA}^0 = 1500\ e^{\left(-\frac{\theta}{81.1}\right)} \qquad (2)$$

where $TrOCA^0$ is tracer TrOCA but without any anthropogenic contribution (Touratier and Goyet, 2004b, Lo Monaco et al., 2005). Assuming that $O_2{}^0 = O_2$ and $TA^0 = TA$ (see the justifications in Touratier and Goyet, 2004b), the estimated concentration of C_{ANT} is given by:

$$C_{ANT} = \frac{TrOCA - TrOCA^0}{1.2} \quad (3)$$

The accuracy of the TrOCA method to compute C_{ANT} is then evaluated by the error propagation technique, as described in detail by Touratier and Goyet (2004b). For each section, the precisions for TCO_2, TA and O_2 measurements are estimated from the averaged standard deviations (µmol kg^{-1}) of properties measured in the core of the North Atlantic Deep Water (NADW; ca. 1700-3500 metres; see Fig. 2):

Section	**σTCO_2**	**σTA**	**σO_2**
EQ99-35°W	8.82	7.71	3.16
EQ99-23°W	5.14	7.45	3.26
EQ99-10/7°W	3.36	5.3	3.28
WOCE A15/94	3.54	2.58	4.27

Using these standard deviations and applying Eqs. 5 to 7 given by Touratier and Goyet (2005), the error on C_{ANT} is calculated for each section (see Fig. 3). When the EQ99 dataset is used, the accuracy of the TrOCA approach improves from west to east (i.e. the error decresases from ~10 µmol kg^{-1} to ~5 µmol kg^{-1}).

Results

Distribution of anthropogenic CO_2

The distributions of C_{ANT} along the three sections 35°W (stations 13 to 47; see Fig. 1), 23°W (stations 48 to 74), and 10°W / 7°W (stations 76 to 93, and 94 to 101) are presented in Fig. 4.

The surface waters belonging to SACW and NACW (South and North Atlantic Central Water; upper 500 m) are characterized by high concentrations of anthropogenic CO_2 (C_{ANT} > 20 µmol kg^{-1}), except at one location (south of 5°S on the section 23°W). High C_{ANT} values in the surface waters of the Atlantic Ocean are expected since this layer is in contact with the atmosphere, which contains high concentrations of anthropogenic CO_2.

Throughout the tropical Atlantic (Fig. 4a to c), the subsurface layer (ca. 500-1200 m) appears to be less contaminated by C_{ANT} (< 20 µmol kg^{-1}). According to Oudot et al. (1999), this portion of the water column is occupied by waters belonging to AAIW (Antarctic Intermediate Water) and UCPW (Upper Circumpolar Water) within the tropics, UCPW being located below AAIW. Both water masses enter the tropics from the southern hemisphere as a narrow north-westward flow along the Brazilian coast (e.g. Wüst, 1935; Reid, 1989; Gordon et al., 1992). The core of these water masses is clearly visible around 4°S on section 35°W (Fig. 4a). As shown by Suga and Talley (1995), these waters extend also eastward along the equator. This is indicated by the presence of low C_{ANT} concentration cores located approximately at 2°S along both sections 23°W and 10°W / 7°W. The AAIW is known to be younger than the UCPW, which reflects different origins (AAIW forms near 45°S within the subantarctic front region, whereas UCPW originates from the Antarctic Ocean). Consequently, the lowest C_{ANT} values within the layer 500-1200 m are probably dominated by the UCPW influence.

Between 1200 m and approximately 4000 m, C_{ANT} increases again with maxima > 20 µmol kg^{-1}. Two main cores of high C_{ANT} values (> 30 µmol kg^{-1}) appear at 2°N and 2°S

along the 35°W section (Fig. 4a). All waters within this layer belong to NADW (North Atlantic Deep Water), which originates from the northern hemisphere. NADW is traditionally subdivided into three components: 1) the UNADW (upper NADW; 1600-1700 m), which is formed in the southern Labrador Sea (LSW; Pickart, 1992); 2) the MNADW (Middle NADW; 2200-3800 m), which is a mixture of LSW and Gibbs Fracture Zone Waters (GFSW); and 3) the LNADW (Lower NADW; around 4000m), which originates from north of the Greenland and the Scotland sills and upstream of the Denmark Strait (Smethie et al., 1986; Schlosser et al., 1991).

All NADW components are transported towards the southern Atlantic by the DWBC. Through its C_{ANT} properties (high values), the DWBC is clearly visible on the 35°W section from 3°S to 1°S, and from 1200 m down to the bottom (Fig. 4a). In this region, UNADW and LNADW are characterized by higher C_{ANT} values than MNADW, which shows a minimum around 3500 m. As noted by Rhein et al. (1995) and Gouriou et al. (1999), the position of the DWBC core at 35°W is highly variable, as it fluctuates between 3°S and 1°30'S. This variability is certainly responsible for the large spot of C_{ANT} contaminated waters around 2°S (Fig. 4a).

There is a strong C_{ANT} gradient within NADW from west to east, with maxima decreasing to less than 25 µmol kg^{-1} on the two most eastern sections. Interestingly, the maximum at 23°W (Fig. 4b) is located south of 4°S, whereas the two maxima appearing along the 10°W / 7°W section (Fig. 4c) are located north of the equator (at 0°30'N and 3°N).

The LNADW core (C_{ANT} > 20 µmol kg^{-1}), which occupies the bottom of the Equatorial Channel at 35°W (around 2°S; Fig. 4a), reaches the 23°W section at approximately 5°S, but with concentrations of C_{ANT} < 10 µmol kg^{-1} (Fig. 4b). This result is in agreement with the earlier conclusion of Andrié et al. (1999) that a topography effect induced by the Paranaiba Ridge (see Fig. 1) deflects the LNADW to the east.

Within the tropics, depths greater than ca. 4500 m are occupied by essentially two bottom waters originating from the southern ocean: the LCDW (Lower Circumpolar Deep Water; Tsuchiya et al., 1994) and the AABW (Antarctic Bottom Water; denser than LCDW). The results of Andrié et al. (1998) suggest that LCDW and AABW, when flowing to the north, would circulate preferentially on the eastern and western side of the Brazil Basin, respectively. Because of the topography, AABW could be blocked at the entrance of the Equatorial Channel (Andrié 1996), whereas LCDW could spread east of the Mid-Atlantic Ridge (MAR) through the Romanche Fracture Zone (RFZ) and the Chain Fracture Zone (CFZ) (Messias et al. 1999). According to several studies (e.g. Rhein et al., 1998; Messias et al. 1999; Andrié et al., 2003), the LCDW is older than the AABW since the latter originates from recently formed Weddell Sea Deep Water (WSDW). Waters of the AABW are thus expected to have a higher C_{ANT} content than those belonging to LCDW.

The results provided by the TrOCA approach for C_{ANT} indicate the presence of AABW on the seafloor of section 23°W, south of 3°S (Fig. 4b). Such a signature is expected since the AABW occupies the bottom of the whole Brazil Basin. Interestingly, deep waters (4000-4500 m) located north of the equator on section 10°W / 7°W (Fig. 4c) could belong to the LNADW (CANT > 10 µmol kg^{-1}). This hypothesis is in agreement with the study made by Messias et al. (1999) which indicates that LNADW and AABW could transit from the Brazil Basin to both the Guinea Basin and the Sierra Leone Basin through the RFZ and the CFZ (Fig. 1).

Comparison with CFC-11 measurements

Anthropogenic tracers like ^3H, $\Delta^{14}C$, or CFCs have been shown to be very useful in understanding the formation of oceanic water masses, their circulation, and their evolution with time (England and Maier-Reimer, 2001). It is often assumed that the distribution of these tracers is similar to that of C_{ANT} because 1) they have been released initially into the atmosphere, and 2) they are conservative like C_{ANT} if we assume that the latter represents a small fraction of the bulk of TCO_2. If this is true, measurements of such tracers could provide independent tools to assess the quality of C_{ANT} distributions.

From the EQ99 cruise, measurements of tracer CFC-11 are available. A detailed analysis of the CFC-11 distribution for EQ99 (Fig. 5) is available in Gouriou et al. (2001), Andrié et al. (2002, 2003), and Freudenthal and Andrié (2002). As in the paper of Andrié et al. (2002), the upper water column (0-1000 m) is not considered here since this layer is characterized by a steep gradient of CFC-11 (from > 2.5 pmol kg^{-1} at the surface to approximately 0.1 pmol kg^{-1} at 1000 m). Consequently, we focus on the comparison between CFC-11 and C_{ANT} for depths > 1000 m.

At depths corresponding to the UNADW, Andrié et al. (2002) identify several CFC-11 cores located at 3°S, 2°S, Eq, 2°N, 4°N and 7°N along the 35°W section (Fig. 5a). The overall distribution of CFC-11 in this layer is in agreement with that of C_{ANT} (compare with Fig. 4). It is not possible however to obtain a close correspondence between distributions of CFC-11 and C_{ANT} for two main reasons: 1) C_{ANT} and CFC-11 sources of emission and air-sea equilibration times greatly differ; and 2) C_{ANT} has increased progressively in the atmosphere for ~130 years, whereas CFC-11 did not begin to increase until the 1930s, in parallel with the sharp increase in industrial activity. For instance, the four CFC-11 maxima, found at 3°S, 2°S, 2°N, and 7°N (Fig. 5a), correspond to four C_{ANT} maxima (see Fig. 4a), but the CFC-11 maxima located at 4°N and especially at the equator have no equivalent in the C_{ANT} distributions. This may result from mixing between different water masses of various ages. As already noted for C_{ANT}, there is also a clear CFC-11 gradient from west to east (Figs. 5a to c). However, the position of the CFC-11 maxima in the UNADW differ from those for C_{ANT} along both 23°W (compare Figs. 4b and 5b) and 10°W / 7°W (compare Figs. 4c and 5c). At 23°W, the CFC-11 maximum is found at 3°S while it is located south of 4°S for C_{ANT}. This indicates that waters of the UNADW south of 4°S are probably older than those found at 3°S. The opposite trend is observed at 10°W / 7°W: waters located north of the equator (where the maxima of C_{ANT} are found) are probably older than those found at 2°S (position of CFC-11 maximum).

As noted in several studies prior to EQ99 (Andrié 1996; Andrié et al., 1998), waters of the MNADW are almost CFC-11 free, except within the DWBC (south of 1°S, section 35°W; see Fig. 5a), where concentrations exceed 0.1 pmol kg^{-1} during EQ99. The level of CFC-11 in the DWBC is much lower in the MNADW (around 2500 m) than in UNADW. When compared to Fig. 4a, the level of C_{ANT} in the MNADW does not radically change from that in UNADW. This may be the result of the greater transit time to reach the tropics for the GFZW (Gibbs Fracture Zone Water, component of the MNADW) than for the more rapidly flowing UNADW: GFZW arriving at low latitudes is contaminated by C_{ANT}, but not entirely by CFC-11 yet.

The CFC-11 signals located south of the equator, and visible at 3500-4000 m on both sections 35°W and 23°W (Figs. 5a and b), indicate the presence of the LNADW (Gouriou et al., 2001). As noted above, in this area along 23°W, the TrOCA approach is in agreement with the CFC-11 results showing a significant C_{ANT} signal for depths > 3500m (Fig. 4b).

On the bottom of section EQ99-10/7°W, the level of CFC-11 in the AABW is low but not negligible (< 0.05 pmol kg^{-1}), as indicated by Fig. 5c (see also Andrié et al. 2003). This is

in agreement with the higher concentration of C_{ANT} found close to the seafloor from the TrOCA approach (Fig. 4c).

Discussion and conclusions

Acting essentially as a source of CO_2 for the atmosphere, the surface layer of the Atlantic Ocean tropical belt cannot accumulate large amounts of C_{ANT}. Throughout the Atlantic Ocean, this anthropogenic tracer is known to accumulate preferentially within the subtropical gyres, where the Ekman convergence is important (Broecker et al., 1985; Sarmiento et al., 1992). Consequently, the levels of C_{ANT} obtained with the TrOCA approach in the surface layer of the tropical belt (up to 70-80 µmol kg^{-1}; Figs. 4 and 6a) are in agreement with the previous work of Touratier and Goyet (2004b).

The TrOCA approach also provides convincing results concerning the bottom distribution (> 4000 m) of C_{ANT} in the southern portion of the 23°W section (Fig. 4b). Like CFC-11, C_{ANT} slightly increases with depth (Figs. 6a and b). This indicates that the TrOCA approach can adequately detect the C_{ANT} signature in the AABW.

The degree of detail reached with the C_{ANT} distribution is comparable to that of the CFC-11. The variability in both the horizontal and the vertical directions reveals numerous structures which are related to the local circulation. This indicates that tracer C_{ANT} could be used like other anthropogenic tracers to track changes in the formation and circulation of the water masses. For instance, it would be interesting to explore the differences of distribution noted between CFC-11 and C_{ANT} in the UNADW of both sections 23°W and 10°W / 7°W. There are mainly three advantages in using C_{ANT} as an anthropogenic tracer: 1) the contamination of oceanic waters by C_{ANT} is much older (it began to increase around the 1870s) and thus gives more informative than tracers ^{3}H, $\Delta^{14}C$ (both tracers dramatically increased in the 1950s after the atmospheric bomb testing) or CFCs; 2) in addition to their own ecological meaning, the measurements of O_2, TCO_2, and TA (i.e. the properties required to compute C_{ANT} with the TrOCA approach) give access to information that is similar to that of other anthropogenic tracers; 3) when the impact of the atmospheric CO_2 excess on ecosystems and the resulting feedbacks are discussed, the utilisation of tracer C_{ANT} is more appropriate than other anthropogenic tracers, which are not directly related to the carbon cycle.

By analyzing several time series available at 35°W from 1992 to 1999, Andrié et al. (1999, 2002) evidenced the continuous increase of the CFC-11 level with time in most water masses. These studies are very useful and informative because they help to understand the way by which the contamination of anthropogenic tracers operates and also the complex patterns of circulation in the area. No doubt further interesting information could be gained by similar work with tracer C_{ANT} (especially where there is no CFCs), depending on the availability of the properties O_2, TCO_2, and TA measured during cruises of the time series.

Both Touratier and Goyet (2004b) and the present contribution estimate the distribution of tracer C_{ANT} by the TrOCA approach and data sets from the Atlantic Ocean (CARINA database and EQ99, respectively). We learn from the former study that the TrOCA approach, when compared to the ΔC^* model of Gruber et al. (1996) and the Chen & Millero approach (Chen and Millero, 1979), provides the most reliable estimate for C_{ANT} throughout the Atlantic Ocean. Although the latter two approaches have been widely applied to compute C_{ANT} in the Atlantic, the Indian, and the Pacific Ocean (e.g. Chen and Pytkowicz, 1979; Chen 1982; Papaud and Poisson, 1986; Poisson and Chen, 1987; Chen et al., 1990; Chen 1993; Goyet and Brewer, 1993; Tsunogai et al., 1993; Chen et al., 1995; Goyet et al., 1998; Gruber 1998; Sabine et al. 1999), it is recommend to revaluate C_{ANT} with the TrOCA approach in the

three oceans, and especially the tropical areas where we observe large differences among results.

The most recent methodologies, like the MIX (Goyet et al., 1999) or the TrOCA approach, should be used conjointly with the less recent ones to assess independently the accumulation of C_{ANT} everywhere in the world ocean. This has been done for the northern Indian Ocean using data of the WOCE I1 cruise by Chalard et al. (submitted). This is the most appropriate way to decrease significantly the large uncertainties that still exist in concentrations of anthropogenic CO_2 and fluxes across the air-sea interface.

Acknowledgements

This work was supported by the ACTION project (Anthropogenic Carbon: Temporal Increase, Observations and Numerization), funded by the French PROOF program (PROcessus biogéochimiques dans l'Océan et Flux). We wish to thank R. Chuchla and D. Ruiz Pino for their leadership with O_2 and CO_2 system properties measurements during the EQUALANT 1999 cruise, respectively. We are also very grateful to B. Schauer for his technical help with CO_2 measurements.

References

Andrié C. (1996). Chlorofluoromethanes in the deep equatorial Atlantic revisited. In: Wefer G., Berger W. H., Siedler G. and D. J. Webb (Eds.), The South Atlantic: present and past circulations. Springer, Berlin, pp. 273-288.

Andrié C., Ternon J. F., Messias M. J., Mémery L. and B. Bourlès (1998). Chlorofluoromethane distributions in the deep equatorial Atlantic during January-March 1993. Deep-Sea Res. I, 45: 903-930.

Andrié C., Ternon J. F., Bourlès B., Gouriou Y. and C. Oudot (1999). Tracer distributions and deep circulation in the western tropical Atlantic during CITHER 1 and ETAMBOT cruises, 1993-1996. J. Geophys. Res., 104: 21195-21215

Andrié C., Rhein M., Freudenthal S. and O. Plähn (2002). CFC time series in the deep water masses of the western tropical Atlantic, 1990-1999. Deep-Sea Res. II, 49: 281-304.

Andrié C., Gouriou Y., Bourlès B., Ternon J. F., Braga E. S., Morin P. and C. Oudot (2003). Variability of AABW properties in the equatorial channel at 35°W. Geophys. Res. Letters, 30: 8007-8010.

Billant A. and P. Branellec (1994). Mesures de salinité et oxygène dissous. In : Recueil de Données, Campagne CITHER 1 : Traceurs Géochimiques, Doc. Scient. ORSTOM Cayenne, N°O.P. 15 : 7-30.

Brewer P.G. (1978). Direct observation of the oceanic CO_2 increase. Geophys. Res. Lett., 5: 997-1000.

Broecker W. S., Takahashi T. and T.-H. Peng (1985). Reconstruction of past atmospheric CO_2 from the chemistry of the contemporary ocean: an evaluation. Tech. Rep. TRO 20, U. S. Dep. of Energy, Washington, D. C.

Chen C.-T. A. and F. J. Millero (1979). Gradual increase of oceanic CO_2. Nature, 277: 205-206.

Chen C.-T. A. and R. M. Pytkowicz (1979). On the total CO_2-titration alkalinity-oxygen system in the Pacific Ocean. Nature, 281: 362-365.

Chen C.-T. A. (1982). On the distribution of anthropogenic CO_2 in the Atlantic and Southern oceans. Deep Sea Res., 29: 563-580.

Chen C.-T. A., Jones E. P. and K. J. Lin (1990). Wintertime total carbon dioxide measurements in the Norwegian and Greenland Seas. Deep Sea Res., 37: 1455-1473.

Chen C.-T. A. (1993). The oceanic anthropogenic CO_2 sink. Chemosphere, 27: 1041-1064.

Chen C.-T. A., Wang S.-L. and A. S. Bychkov (1995). Carbonate chemistry of the Sea of Japan. J. Geophys. Res., 100: 13737-13745.

DOE (1994). Handbook of methods for the analysis of the various parameters of the carbon dioxide system in sea water; version 2, A. G. Dickson and C. Goyet (Eds.), ORNL/CDIAC-74.

England M. H. and E. Maier-Reimer (2001). Using chemical tracers to assess ocean models. Rev. Geophysics, 39: 29-70.

EQUALANT 99 Cruise Report (2000). Campagne EQUALANT 99. Rapport de campagne à la mer. Rapport Interne LODYC n°2000-01, http://nansen.ipsl.jussieu.fr/EQUALANT/.

Fournier P., Oudot C. and F. Baurand (1997). Mesures d'oxygène dissous, Campagne ETAMBOT 1, Recueil de données, Vol 2/2. Doc. Scient. ORSTOM Cayenne, N°O.P. 23.

Freudenthal S. and C. Andrié (2002). The arrival of a "new" Labrador Sea Water signal in the tropical Atlantic in 1996. Geophys. Res. Letters, 29: 1741-1744.

Gordon A. L., Weiss R. F., Smethie W. M. Jr. and M. J. Warner (1992). Thermocline and intermediate communication between the South Atlantic and Indian Oceans. J. Geophys. Res., 97: 7223-7240.

Gouriou Y., Bourlès B., Mercier H. and R. Chuchla (1999). Deep jets in the equatorial Atlantic Ocean. J. Geophys. Res., 104: 21217-21226.

Gouriou Y., Andrié C., Bourlès B., Freudenthal S., Arnault S., Aman A., Eldin G., Penhoat U. du, Baurand F., Gallois F. and R. Chuchla (2001). Deep circulation in the equatorial Atlantic Ocean. Geophys. Res. Letters, 28 : 819-822.

Goyet C. and P. G. Brewer (1993). Biochemical properties of the oceanic carbon cycle. In: J. Willebrand and D.L.T. Anderson (Editors), Modelling Oceanic Climate Interactions. NATO ASI Series, I 11, Springer-Verlag, Berlin, Heidelberg, pp. 271-297.

Goyet C., Adams R. and G. Eisched (1998). Observations of the CO_2 system properties in the tropical Atlantic Ocean. Mar. Chem., 60: 49-61.

Goyet C., Coatanoan C., Eischeid G., Amaoka T., Okuda K., Healy R. and S. Tsunogai (1999). Spatial variation of total alkalinity in the northern Indian Ocean: a novel approach for the quantification of anthropogenic CO2 in seawater. J. Mar. Res., 57: 135-163.

Gruber N., Sarmiento J.L. and T.F. Stocker (1996). An improved method for detecting anthropogenic CO_2 in the oceans. Glob. Biogeochem. Cycles, 10: 809-837.

Gruber N. (1998). Anthropogenic CO_2 in the Atlantic Ocean. Glob. Biogeochem. Cycles, 12: 165-191.

Lo Monaco C., Goyet C., Metzl N., Poisson A. and F. Touratier (in press). Distribution and inventory of anthropogenic CO2 in the southern ocean: comparison of three data-based methods. J. Geophys. Res.

Maier-Reimer E. (1993). Geochemical cycles in an ocean general circulation model: preindustrial tracer distributions. Glob. Biogeochem. Cycles, 7: 645-677.

Messias M.J., Andrié C., Mémery L. and H. Mercier (1999). Tracing the North Atlantic Deep Water through the Romanche and Chain fracture zones with chlorofluoromethanes. Deep-Sea Res. I, 46: 1247-1278.

Oudot C. and C. Andrié (1986). Variabilité des pressions partielles de CO_2 océanique et atmosphérique dans l'Atlantique tropical. Oceanologica Acta, 9 : 169-177.

Oudot C., Ternon J. F., Andrié C., Braga E. S. and P. Morin (1999). On the crossing of the equator by intermediate water masses in the western Atlantic Ocean: identification and pathways of Antarctic Intermediate Water and Upper Circumpolar Water. J. Geophys. Res., 104: 20911-20926.

Papaud A. and A. Poisson (1986). Distribution of dissolved CO2 in the Red Sea and correlation with other geochemical tracers. J. Mar. Res., 44: 385-402.

Peng T.-H., Wanninkhof R., Bullister J. L., Feely R. A. and T. Takahashi (1998). Quantification of decadal anthropogenic CO_2 uptake in the ocean based on dissolved inorganic carbon measurements. Nature, 38: 560-563.

Pickart R. S. (1992). Water mass components of the North Atlantic deep western boundary current. Deep-Sea Res., 39: 1553-1572.

Poisson A. and C.-T. A. Chen (1987). Why is there little anthropogenic CO_2 in the Antarctic Bottom Water? Deep Sea Res. A, 34: 1255-1275.

Reid J. L. (1989). On the total geostrophic circulation of the South Atlantic Ocean: flow patterns, tracers and transports. Prog. Oceanogr., 23: 149-244.

Rhein M., Stramma L. and U. Send (1995). The Atlantic deep western boundary current: water masses and transports near the equator. J. Geophys. Res., 100: 2441-2457.

Rhein M., Stramma L. and G. Krahmann (1998). The spreading of Antarctic bottom water in the tropical Atlantic. Deep-Sea Res. I, 45: 507-527.

Sabine C. L., Key R. M., Johnson K. M., Millero F. J., Poisson A., Sarmiento J. L., Wallace D. W. R. and C. D. Winn (1999). Anthropogenic CO_2 inventory of the Indian Ocean. Glob. Biogeochem. Cycles, 13: 179-198.

Sarmiento J. L., Orr J. C. and U. Siegenthaler (1992). A perturbation simulation of CO_2 uptake in an ocean general circulation model. J. Geophys. Res., 97: 3621-3645.

Sarmiento J. L., Murnane R. and C. Le Quéré (1995). Air-sea CO_2 transfer and the carbon budget of the North Atlantic. Philos. Trans. R. Soc. London, B, 348: 211-219.

Schlosser P., Bonisch G., Rhein M. and R. Bayer (1991). Reduction of deepwater formation in the Greenland sea during the 1980s: evidence from tracer data. Science, 251: 1054-1056.

Smethie W. M., Ostlund H. G. and H. H. Loosli (1986). Ventilation of the deep Greenland and Norwegian seas: evidence from krypton-85, tritium, carbon-14 and argon-39. Deep-Sea Res. A, 33: 675-703.

Stocker T. F., Broecker W. S. and D. G. Wright (1994). Carbon uptake experiments with a zonally averaged global circulation model. Tellus B, 46: 103-122.

Suga T. and L. D. Talley (1995). Antarctic Intermediate Water circulation in the tropical and subtropical South Atlantic. J. Geophys. Res., 100: 13441-13453.

Takahashi T., Sutherland S. C., Sweeney C. et al. (2002). Global sea-air CO_2 flux based on climatological surface ocean pCO2, and seasonal biological and temperature effects. Deep Sea Res. II, 49: 1601-1622.

Touratier F. and C. Goyet (2004a). Definition, properties, and Atlantic Ocean distribution of the new tracer 'TrOCA'. J. Mar. Syst.,46: 169-179.

Touratier F. and C. Goyet (2004b). Applying the new TrOCA approach to assess the distribution of anthropogenic CO_2 in the Atlantic Ocean. J. Mar. Syst.,46: 181-197.

Tsuchiya M., Talley L. D. and M. S. McCartney (1994). Water-mass distributions in the western South Atlantic: a section from South Georgia Island (54S) northward across the equator. J. Mar. Res., 52: 55-81.

Tsunogai S., Ono T. and S. Watanabe (1993). Increase in total carbonate in the Western North Pacific water and a hypothesis on the missing sink of anthropogenic carbon. J. Oceanogr., 49: 305-315.

Weiss R. F., Bullister J. L., Gammon R. H., and M. J. Warner (1985). Atmospheric chlorofluoromethanes in the deep equatorial Atlantic. Nature, 314: 608-610.
WOCE handbook (1994). WOCE operations manuel. Vol. 3, Part 3.1.3.: WHP operations and methods. WHP Office Report WHPO 91-1, WOCE report N°68/91, Revision 1.
Wüst G. (1935). Schichtung und zirkulation des Atlantishen Ozeans. Die Stratosphäre, in Wissenschaftliche Ergebnisse der Deutschen Atlantischen Expedition auf dem Forschungs – und Vermessungsschiff „Meteor“ 1925-1927, vol. 6, Walter de Gruyter, Berlin, pp. 109-288.

Figure Captions

Figure 1: Map showing the tropical Atlantic Ocean bathymetry and the stations of the EQUALANT 1999 cruise (EQ99). The three sections at 35°W (called EQ99-35°W; stations 13 to 47), 23°W (called EQ99-23°W; stations 48 to 47), and 10°W / 7°W (called EQ99-10/7°W; stations 76 to 101) are used to draw the distribution of the properties. The section of the WOCE A15 cruise sampled in 1994 (called WOCE A15/94; dashed line) is also indicated. (RFZ: Romanche Fracture Zone; CFZ: Chain Fracture Zone).

Figure 2: Section average profiles for a) O_2; b) TCO_2; and c) TA.

Figure 3: Accuracy of the TrOCA method. The error on anthropogenic CO_2 (C_{ANT}) is estimated for each section.

Figure 4: Distribution of the anthropogenic CO_2 (C_{ANT}) as computed from the TrOCA approach. a): at 35°W; b) at 23°W; and c) at 10° / 7°W.

Figure 5: Distribution of the CFC-11 concentration. a): at 35°W; b) at 23°W; and c) at 10° / 7°W.

Figure 6: All sections together, vertical distribution of a) C_{ANT} computed from the TrOCA approach and b) the CFC-11 concentrations.

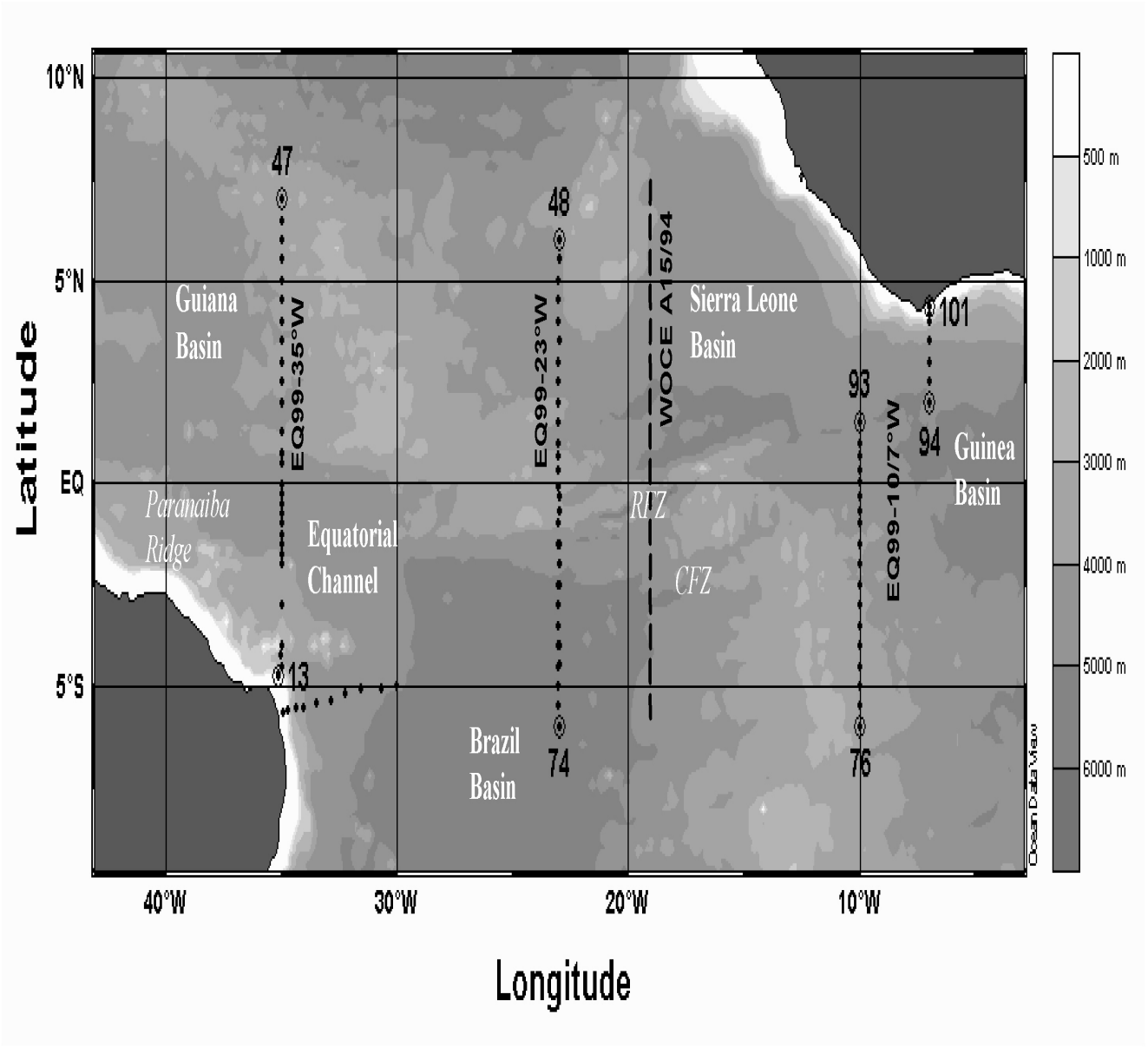
10°N
5°N
EQ
5°S
Latitude
40°W
30°W
20°W
10°W
Longitude
47
48
13
74
93
94
101
76
EQ99-35°W
EQ99-23°W
WOCE A15/94
EQ99-10/7°W
Guiana Basin
Sierra Leone Basin
Guinea Basin
Brazil Basin
Paranaiba Ridge
Equatorial Channel
RTZ
CFZ
500 m
1000 m
2000 m
3000 m
4000 m
5000 m
6000 m
Ocean Data View

Fig. 1

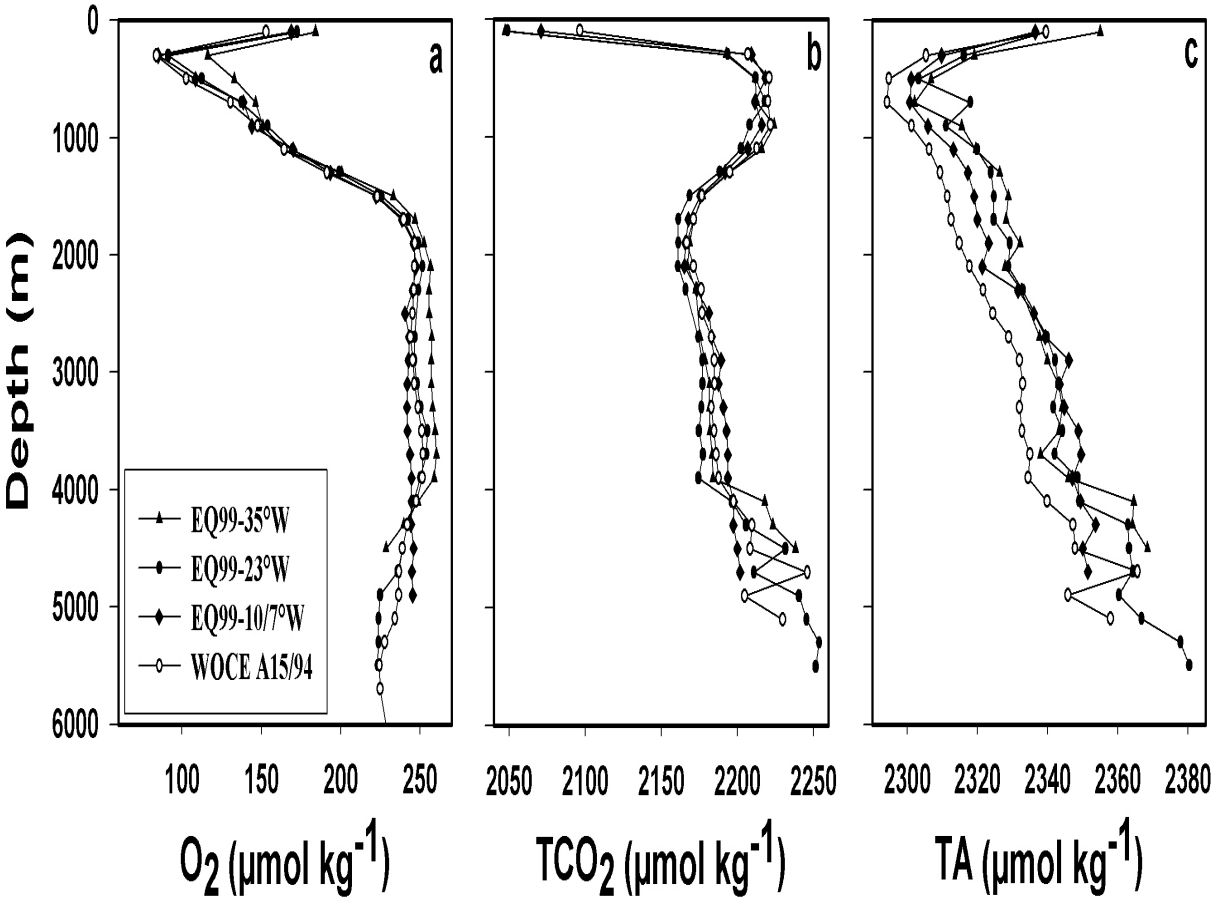
Depth (m)
0
1000
2000
3000
4000
5000
6000
a
b
c
EQ99-35°W
EQ99-23°W
EQ99-10/7°W
WOCE A15/94
100
150
200
250
2050
2100
2150
2200
2250
2300
2320
2340
2360
2380
O2 (µmol kg-1)
TCO2 (µmol kg-1)
TA (µmol kg-1)

Fig. 2

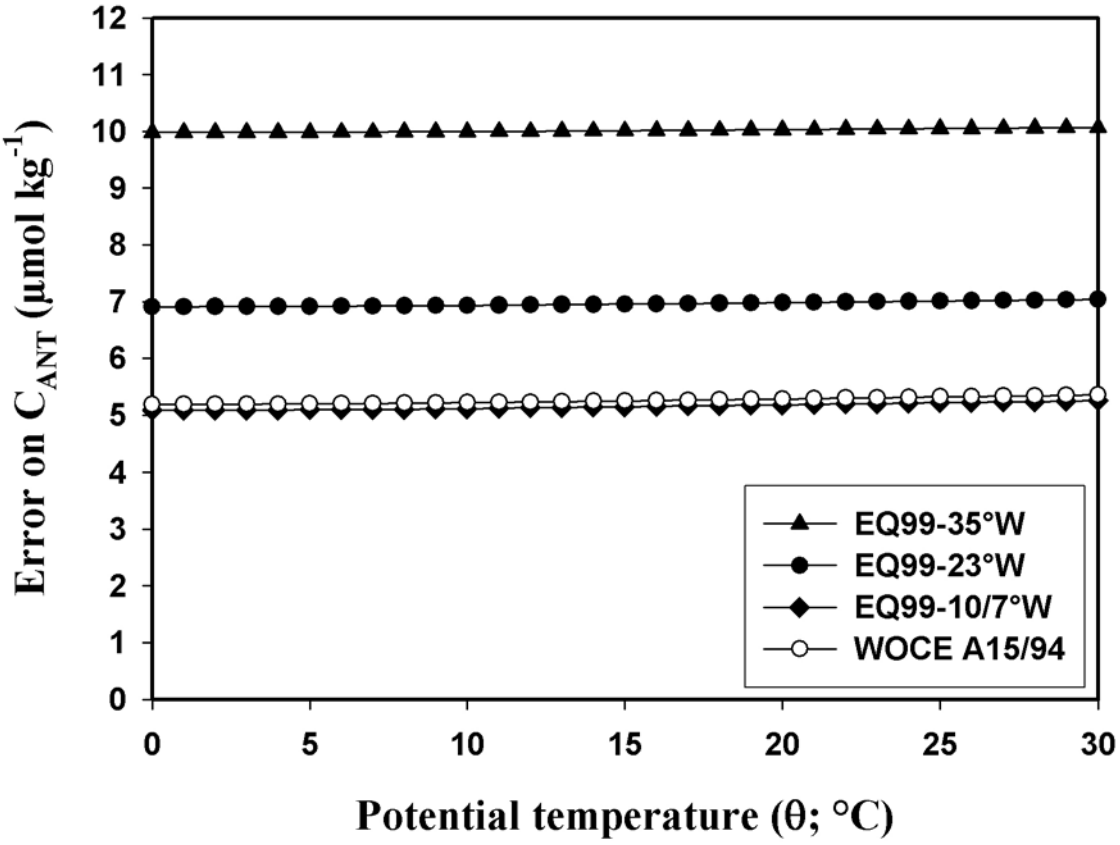
Error on C_{ANT} (μmol kg^{-1})
Potential temperature (θ; °C)
EQ99-35°W
EQ99-23°W
EQ99-10/7°W
WOCE A15/94
0
1
2
3
4
5
6
7
8
9
10
11
12
0
5
10
15
20
25
30

Fig. 3

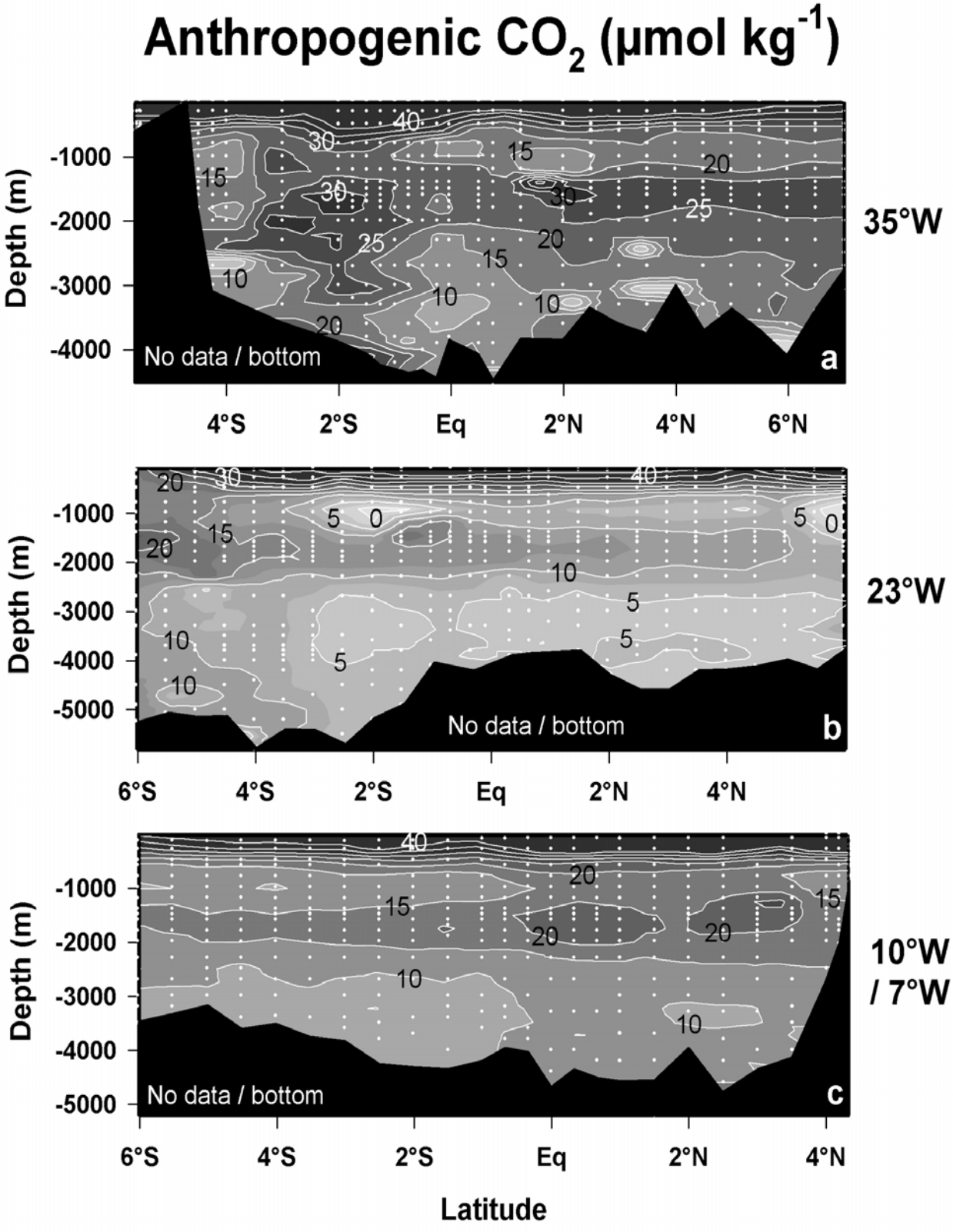
Anthropogenic CO_2 (µmol kg^{-1})
Depth (m)
-1000
-2000
-3000
-4000
-5000
No data / bottom
a
35°W
4°S
2°S
Eq
2°N
4°N
6°N
b
23°W
6°S
c
10°W
/ 7°W
Latitude

Fig. 4

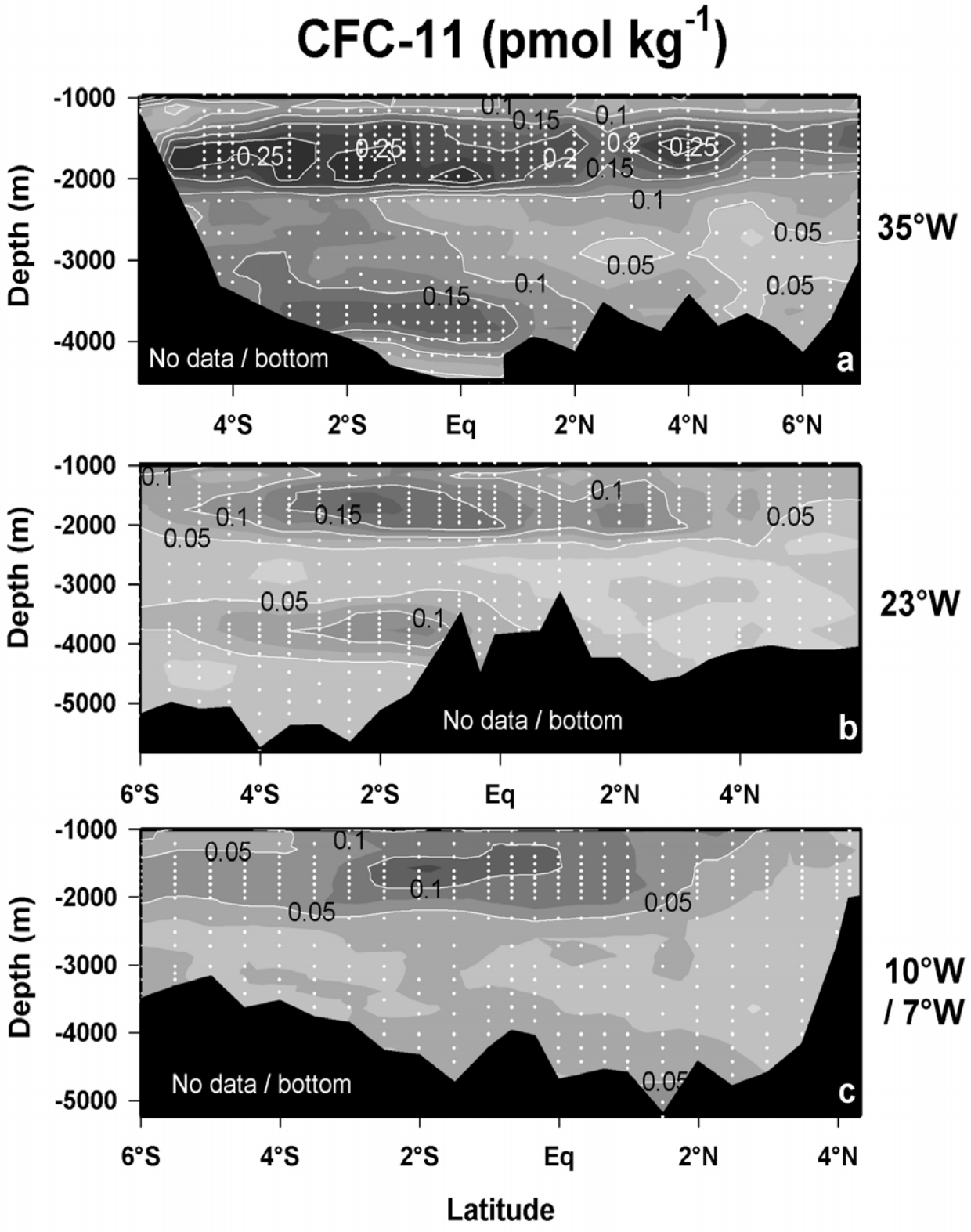
CFC-11 (pmol kg-1)
Depth (m)
-1000
-2000
-3000
-4000
-5000
No data / bottom
a
b
c
35°W
23°W
10°W
/ 7°W
4°S
2°S
Eq
2°N
4°N
6°N
6°S
Latitude

Fig. 5

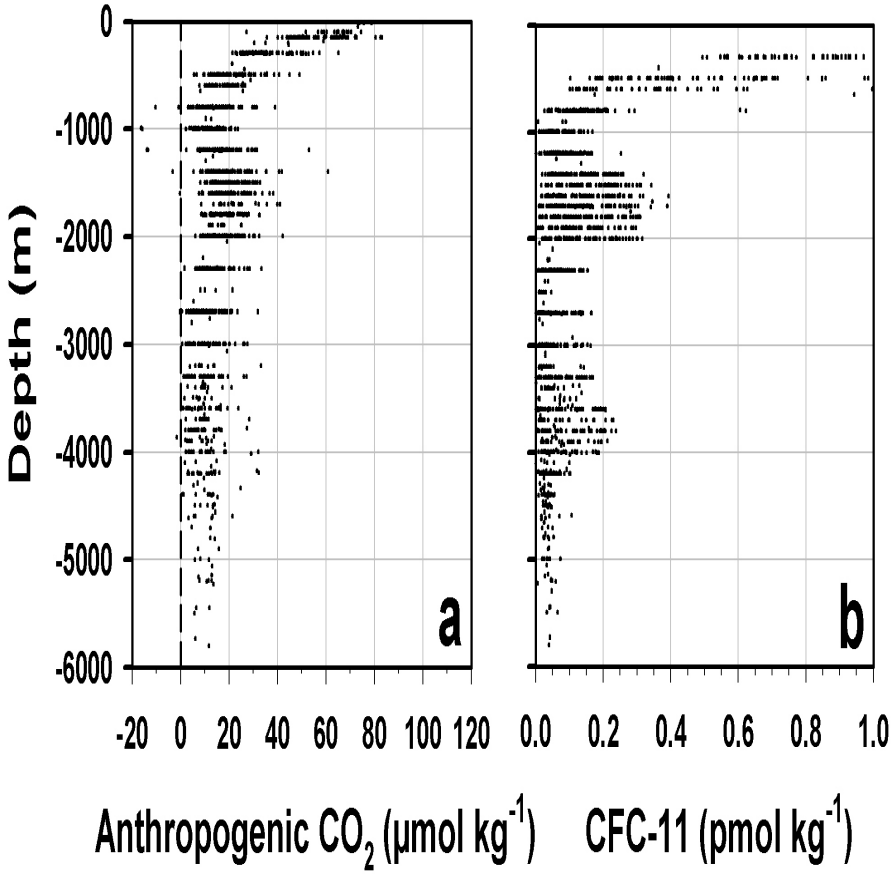
0
-1000
-2000
-3000
-4000
-5000
-6000
Depth (m)
a
b
-20 0 20 40 60 80 100 120
0.0 0.2 0.4 0.6 0.8 1.0
Anthropogenic CO_2 (µmol kg^{-1})
CFC-11 (pmol kg^{-1})

Fig. 6